LAWRENCE
LIVERMORE
NATIONAL
LABORATORY

Possible Laminographic and Tomosynthesis Applications for Wolter Microscope Scan Geometries

D. Schneberk, J. Jackson, H. Martz

October 13, 2004

Disclaimer

Possible Laminographic and Tomosynthesis Applications for Wolter Microscope Scan Geometries[1]

Daniel Schneberk, Jessie Jackson and Harry Martz

UCRL-#

Lawrence Livermore National Laboratory

The Wolter microscope includes a number of attractive features for x-ray imaging, and possible connections to laminographic and tomosynthesis 3D object recovery algorithms. This type of instrument employs x-ray optics to sift out single energy x-rays from a broader spectral energy source, and direct those x-rays to a "focus plane" similar to the operation of a optical microscope (see Figure 1 for schematic of a Wolter instrument). Unlike optical microscopes the 3D object can be thick in the direction of the x-rays and in this case more of the intensity of the image is affected by the out-of-focus planes, since the ray-paths span the entire depth of the object. It is clear that the "in-focus" plane of a Wolter contain more 3D information than a simple "point-projection" radiograph. However, it is not clear just how the impact of the out-of-focus planes obscures or distorts features of interest for the in-focus planes. Further, it is not clear just how object positioning can be combined with multiple acquisitions to enable recovery of other planes within the object function or the entire object function.

Of particular interest here are Wolter microscopes configured for mesoscale objects (mm extent with um features). Laminographic and tomosynthesis scanning methods can be strategic for this type of inspection instrument. First, photon output for inspection purposes can be meager in this type of "small field of view" system. With laboratory x-ray sources a single image can require up to 10 minutes to accumulate adequate signal. Techniques that can obtain 3D object information from small numbers of views, rotational or translational, are consequently at a premium. Laminographic and tomosynthesis scanning methods require relatively small numbers of views (2-30). Secondly, the Wolter microscope scan geometry in a single view is a fit with the type of source-detector geometry achieved through source-object-detector re-positioning in laminographic and tomosynthesis systems. Figure 2 contains a picture of the Wolter optics geometry for inspection. Figure 3 contains an illustration of the scan geometry used in single-plane laminography for flat objects, while figure 4 contains a picture of the scan geometry and motion for a class of tomosynthesis algorithms. The Wolter transmission paths depicted in figure 2 are similar to laminographic and tomosynthesis paths and they provide opportunities to exploit either of these algorithms for removing out of plane blur from Wolter optic images.

Other algorithms may arise from the sequence of images obtained by translation through the focus of the Wolter microscope. A variety of LLNL programs have developed iterative and semi-iterative schemes for utilizing prior knowledge from drawings, or other physical measurements to improve defect recognition and inspection of objects. One such algorithm would use the laminographic estimate of each plane as the first estimate of the object function, then iterate on the object function until the forward projections match the acquired sequence of projections translated through the focus of the Wolter microscope.

Unlike the laminography and tomosynthesis approaches this particular approach requires a forward model of the projection through the object.

We employed an LLNL developed Wolter simulation code [Jackson 2004] to evaluate possible scanning options since a working Wolter was not available. Six synthetic objects were formulated: 1) concentric spheres with a cylindrical void (see Figure 5), 2) concentric spheres with a cylindrical inclusion (see Figure 5), 3) a sphere with a number of successively smaller sphere-voids arranged in the mid-plane of the object (See Figure 6), 4) a sphere with a number of successively smaller sphere inclusions arranged in the mid-plane of the object (see Figure 6), 5) a slab object with voids at the entrance plane and at the exit plane of the thickness, and 6) a slab object with inclusions at the entrance plane and at the exit plane of the thickness. Of the six synthetic objects only the middle two (the sphere with different size spheres arranged at the mid-plane) were studied extensively.

A number of scan regimes were specified for simulation. First, we simulated "translation through focus" scanning. For this type of scan regime the object was placed at focus and moved in small increments towards the detector. An illustration of this type of scanning is shown in Figure 7. The second scan mode is rotation of the object. The third scan mode is horizontal and vertical translation of the object. These three motions taken together would enable any of the possible scan trajectories for various algorithms (including CT) to be implemented. Termination of the LDRD SI project allowed only the first scan mode to be implemented and simulations generated.

Fundamentals of Laminography and tomosynthesis

A schematic of the generalized coordinates for laminography and tomosynthesis is given in Figure 7.[Bossi, et al. 2002] The purpose of any of the different algorithms is by accumulation or by differencing isolate a particular plane in focus for a certain scan sequence. In the single plane laminography case the source, $\mathbf{S}$-> (XS_k, YS_k, ZS_k) and detector $\mathbf{d}$-> (Xd_k, Yd_k, Zd_k) are shifted by a certain angle, where k indexes the images. Using the positions of $\mathbf{S}$ and $\mathbf{d}$ for images $\mathbf{A}$ and $\mathbf{B}$ (see Figure 3), we can solve a linear equation for the shift in the images required to add/subtract those pixels from the two images that involve the same coordinates for a particular plane. The $(A + B) - |(A - B)|$ image effectively emphasizes the object information for a plane in the object. The addition of the two images, $(A + B)$, combines both infocus and blurred features from both images. The absolute value difference of the two images, $|(A - B)|$, removes the features that are in focus. For $(A + B) - |(A - B)|$ features not in the same position on the images (not in focus) will be removed and those in focus will be emphasized.

Tomosynthesis algorithms incorporate a range of scanning motions and 10-30 images to generate images of 3D object features. In these algorithms we define a plane of interest in the object function and solve for coordinates of the detector measurements intersecting those voxels at that plane connected along ray-path lines to the x-ray source. The exact details of the algorithm depend upon the motion of the source and detector and the number of views acquired. In many ways there is a continuum for object recovery algorithms, beginning with laminography to obtain information on a few planes, to tomosynthesis which obtains information on a larger number of planes of the object, to full 3D Computed Tomography.

It should be mentioned here that we are not getting a 3D quantitative image of the internals of the object commensurate with 3D computed tomography. One of the important characteristics of the CT reconstructed image is the near equivalence of the point spread function in any direction around object features. This is not the case for laminography and tomosynthesis, since there are a number of planes that are not imaged well. The planes that are orthogonal to the axis of movement for the source and detector have a blur function much larger than the plane identified in Figures 3 and 4. However, there is genuine 3D object information in laminographic and tomosynthesis images although you may not get an accurate dimension for the features of interest.

The geometry of the Wolter microscope includes many possibilities for this type of operation. First, consider the sequence of images obtained from "translation through focus". The plane in focus is only partly influenced by the out of focus features. As is the case with microscopy the difference between two images at different planes of focus can remove the out-of-focus planes in the object. In the same way, for large depth of field systems, features enclosed by the depth of field will subtract out for small translation through focus movements. The point at which a feature is revealed in the difference image relates to the 3D size of the object.

Results from first set of simulations

The sphere with the voids (Figure 6) provides an interesting example of the properties of the Wolter microscope. A selection of Wolter microscope simulated images with the object centered at the focal plane and at different distances from the focal plane are given in Figure 8. Difference, (A – B) images where A is the image for the object at the focal plane and B is where the center of the object is located at 0.5, 2.5 and 5.0 um from the focal plane in the direction of the detector are shown in Figure 9. Notice there is almost no difference for the 0.5-um difference image. Secondly, notice the larger voids show some change in imagery for the small translation movements indicating some change in object function over that translated distance for the focal length of this simulated Wolter. Lastly, notice the indication of the small 1 um holes at the 2.5 um difference, and the clear identification of the 1 um holes for the 5 um difference image. Consequently, from these few images we can surmise the depth of the small features (less then 2.5 um), and their size in the horizontal dimension. In similar fashion we can get a size estimate of the depth of each of the larger features. Figure 10 contains small (0.5 μm) difference images at 10, 15 and 20 um from the focal plane. These small difference images show progressively little change as the distance from the focal plane increases. However this is in contrast to the large changes that occur when you take the difference of two images where one is the focal plane and the other is far fro the focal plane.

A sequence of difference images need to be further investigated:

- Any given image subtracted from the rest;

- Every image minus the image that is a depth of focus away;

- Every image minus it's adjacent image.

It also is useful to further study summary statistics (minimum, maximum and median) for these sequences of difference images. The sequences of difference images may provide a initial conditions for a CCG-type iterative reconstruction of the object function. We think

the difference images could provide first estimates of the position and size of different features and enable a faster convergence.

Time did allow us to implement the other scan modes, i.e., rotating the object function, horizontal translation of the object function and translating the object in height. It is recommended that these changes be made to the Wolter simulation code if the work resumes and those scan modes simulated as a first priority.

Summary

A Wolter Optics instrument provides a number of interesting opportunities for laminographic or tomosynthesis techniques. The nature of the Wolter inspection geometry resembles the geometry of the source and detector positions for some of the common laminographic and tomosynthesis modes. Using the LLNL Wolter simulation code a number of simulations were performed. A number of scan modes were slated for implementation: 1) translation through the focal plane, 2) object rotation, 3) horizontal translation, and 4) translation in height. Of these different modes only the translation through the focal plane mode was implemented. A number of different objects were designed to evaluate the inspection properties of the Wolter instrument. Three different types of objects were proposed, 1) objects with fine and coarse detail at the mid-plane, 2) objects with features throughout the object function, and 3) for the other two types, objects with highly attenuating features in the object functions. Of these different types of objects only the first type was simulated.

From the "translation-through-focal-plane" images of the object with features on the mid-plane a number of calculations were performed. These calculations consisted of sequence of difference images, the difference between a single image and the rest of the images in the sequence, and differences between adjacent images. Features smaller than the "in-focus" width of the instrument required a difference with an image translated greater than a "focus-width" to identify the features. These coarse estimates of feature position and size can provide the starting point for CCG-type iterative codes. While the "depth" inspection accuracy of the Wolter microscope is heavily influence by the "focus width", it does provide a way to obtain 3D information in a few images.

Future Work

A number of possible scan modes remain untested and could be evaluated with the implementation of new features in the simulator. Upon resumption of this work we recommend the following steps be pursued first: 1) the Wolter simulator be upgraded to include all of the scan modes identified, horizontal translation, vertical translation, through-focus, and object rotation, 2) all of the objects mentioned above be simulated especially the "slab" objects which include features at a distance larger than the focus-width of the Wolter.

References

Bossi, Richard, Iddings Frank, Wheeler George C, and Patrick Moore, <u>NonDestructive Testing Handbook</u>, 3rd Edition, Volume 4, Radiographic Testing,, Chap12, Figure 5, pg 307, 2002 ASNT.

Jackson, J. A., (2004), "Wolter X-ray Microscope Computed Tomography Ray-Trace Model with Preliminary Simulation Results," Lawrence Livermore National Laboratory, Livermore, CA, UCRL-TR-206864.
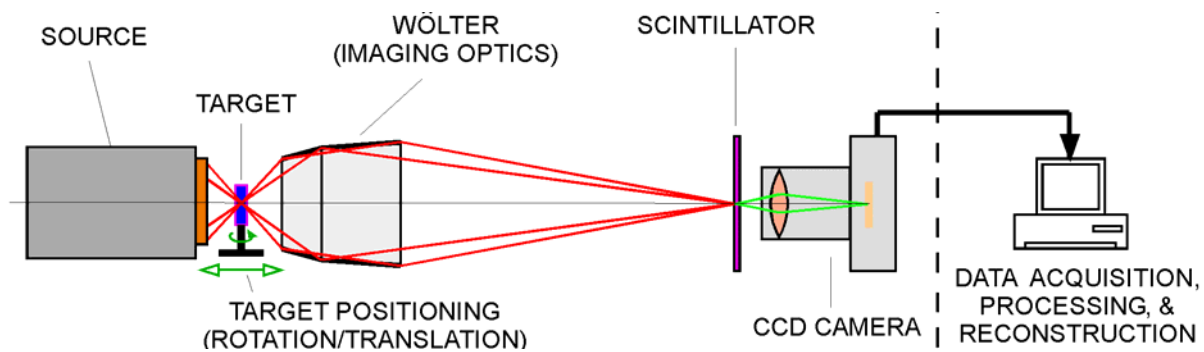
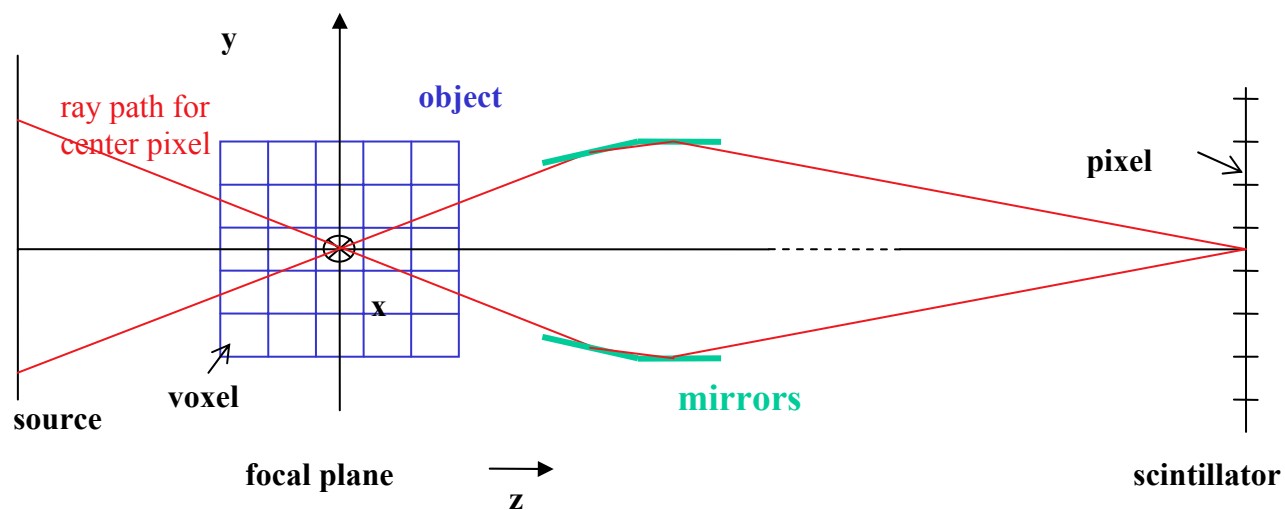**Figure 1 – Schematic of Wolter x-ray optics and x-ray microscope system components.**

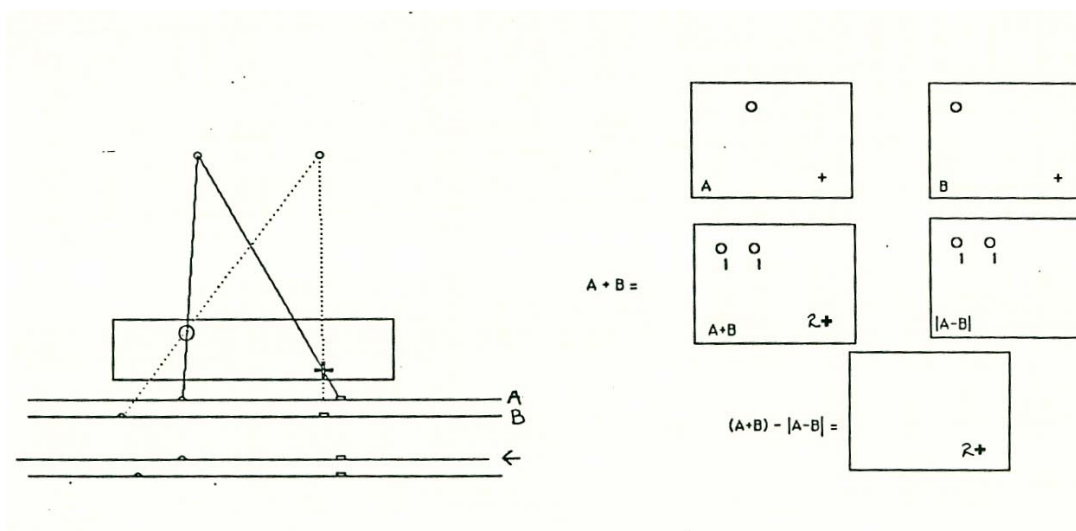**Figure 2 – Schematic of Wolter x-ray optic geometry used in the simulation studies.**

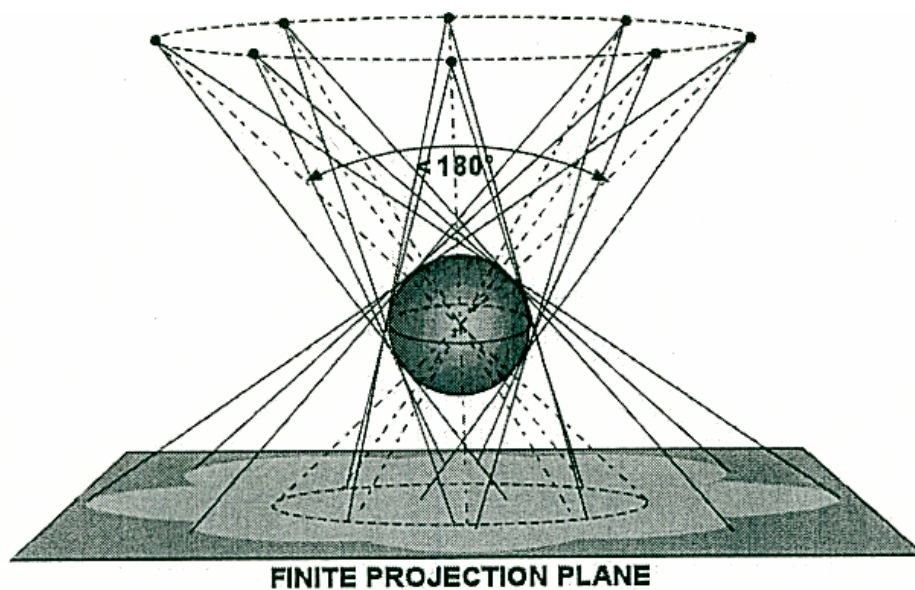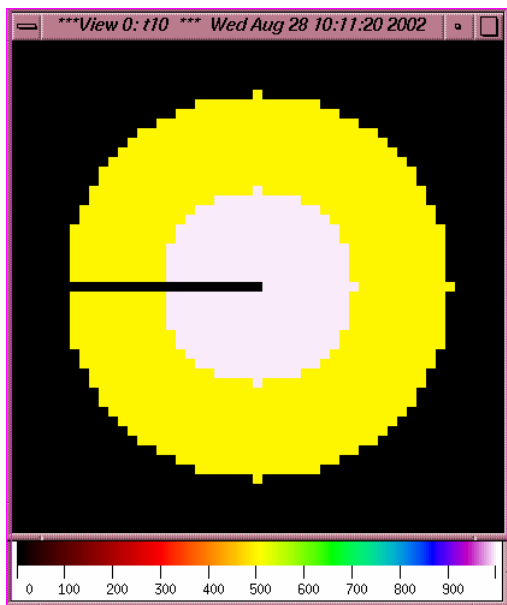**Figure 3 – Example of single plane laminography for standard point projection scanning.**

FINITE PROJECTION PLANE

Figure 4 – Example of tomosynthesis scanning geometry for point projection source.

Object
Each voxel is 0.002 x 0.002mm x 0.002mm
This object in this test is 51 x 51 x 51 voxels or
  0.102mm x 0.102mm x 0.102mm
Two concentric spheres
  • **sphere 1 – radius = 10 voxels = 0.02mm; value = 1000**
  • **sphere 2 – radius = 20 voxels = 0.04mm; value = 500**
a line of value 0 is placed on the center slice of the object
from (0, 25, 25) to (25, 25, 25)

Scintillator
51 x 51 pixels; pixel = 0.024mm
1.224 mm x 1.224 mm
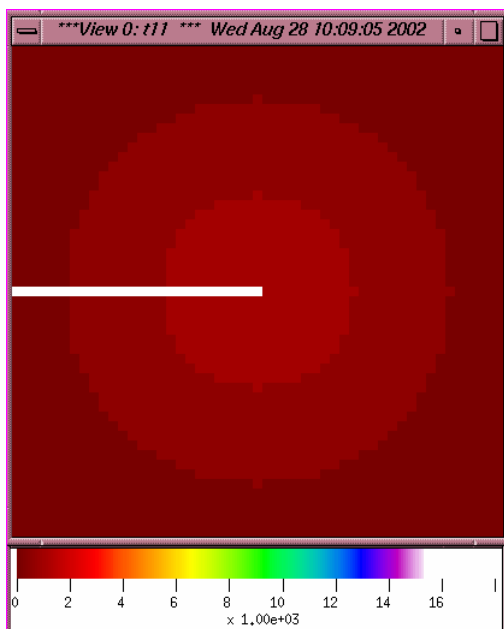
The test is run by placing the
object so the front face is on the
focal plane, the object is
then stepped along the z-axis until
the back face is on the focal plane

Figure 5 – First set of simulated objects – concentric spheres one with a cylindrical void (top) and one with a cylindrical inclusion (bottom) – for Wolter forward projection.
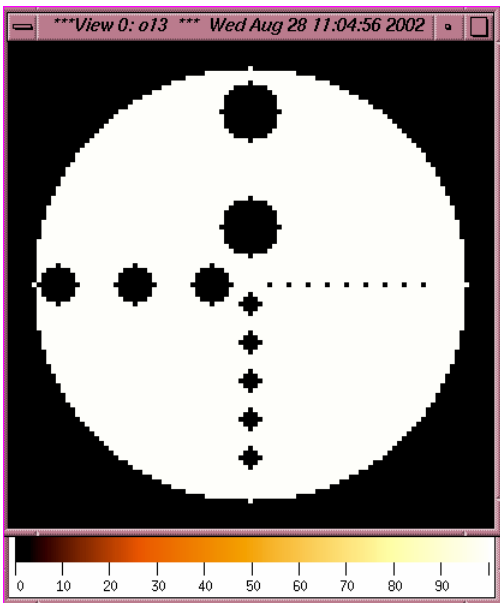
Object
Each voxel is 0.0005 mm x 0.0005 mm x 0.0005 mm
This object in this test is 101 x 101 x 101 voxels or
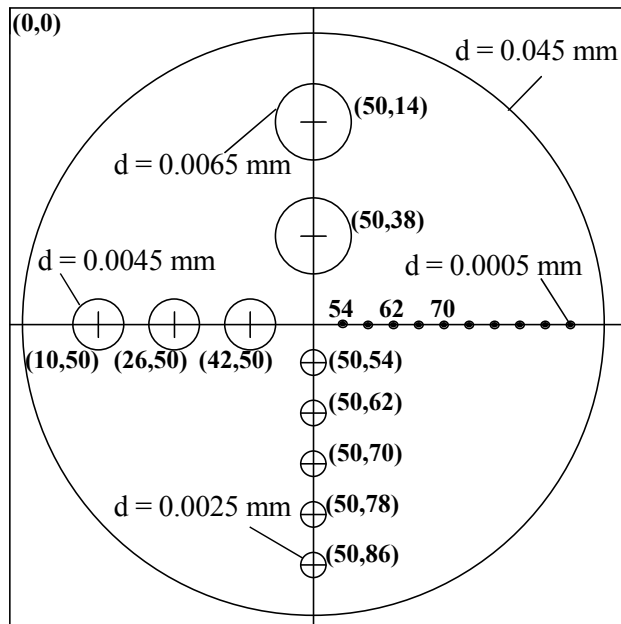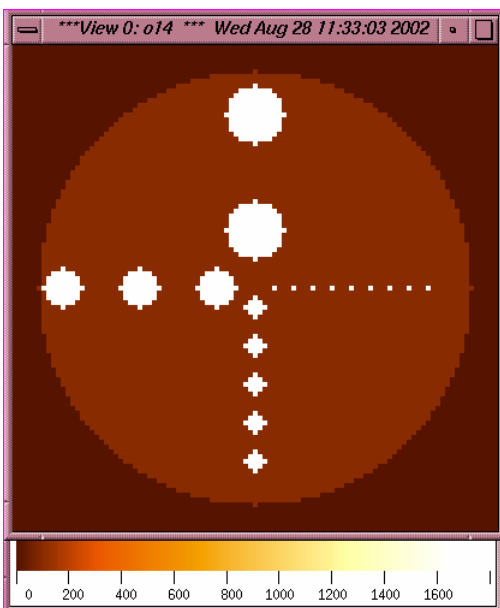 **0.0505 mm x 0.0505 mm x 0.0505 mm**
One sphere
  - **radius = 45 voxels = 0.0225 mm; value = 100**
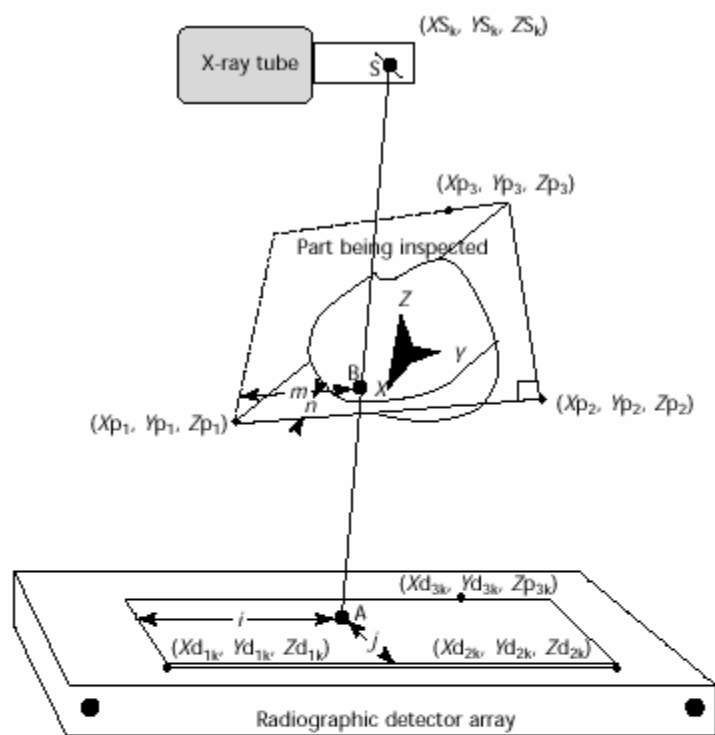**Spherical voids are placed as shown in the diagram**

Scintillator
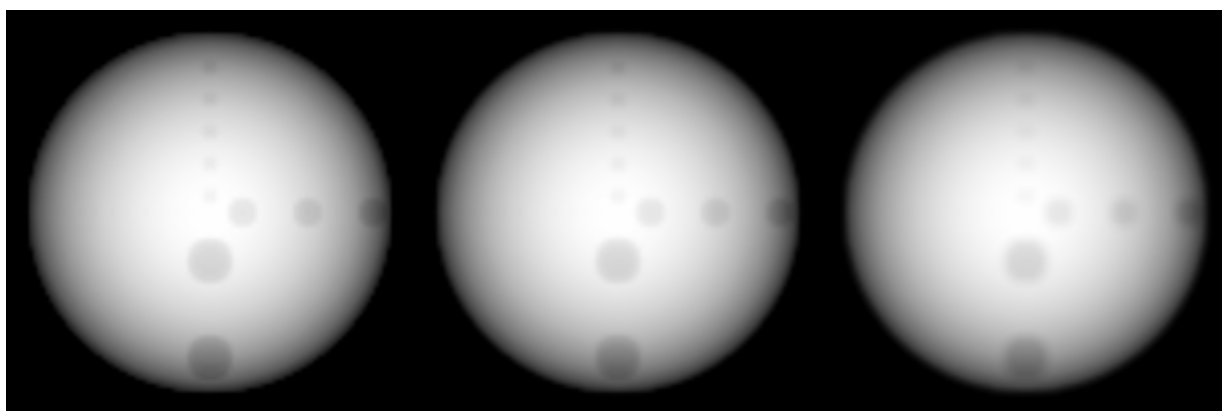**101 x 101 pixels; pixel = 0.006 mm**
0.606 mm x 0.606 mm

Figure 6 – Details of a simulated sphere with voids (top) or inclusions (bottom) on the object center plane.
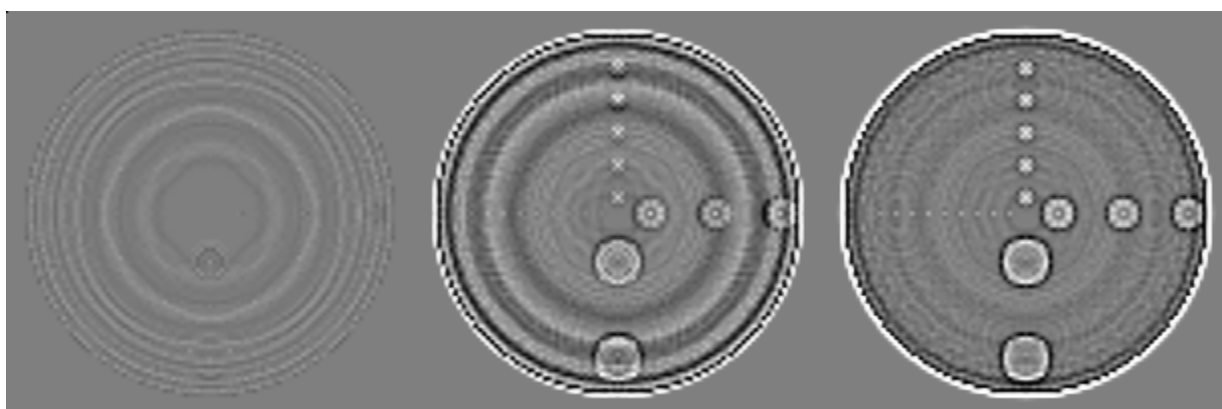
Figure 7 –Generalized coordinates for obtaining laminographic images from sequences of images acquired at different source-detector positions.
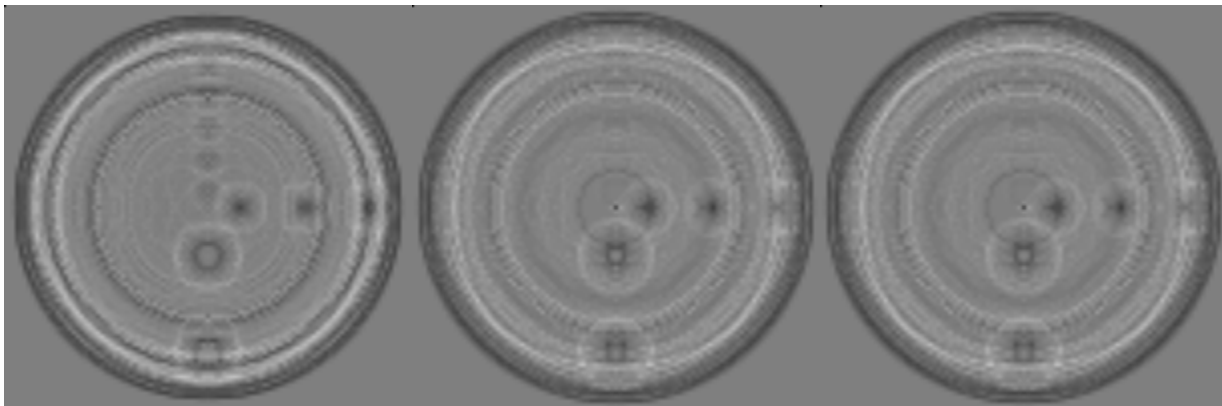
Object at Center Focus   Object @ 2.5 um shift   Object @ 5 um shift

Figure 8 – Three views of the sphere with voids. Each image is for the center of the object at a different locations from the focal plane as labeled.

Difference of 0 & 0.5um   Difference of 0 & 2.5um   Difference of 0 & 5um

Figure 9 – Difference images of mid-plane focus to other translated views.

Difference 10&10.5 um   Difference of 15&15.5 um   Difference of 20&20.5 um

Figure 10 – Difference of adjacent images from sequence of "thru-focus" images.